Pergamon

Cement and Concrete Research, Vol. 25, No. 3, pp. 561-571, 1995

0008-8846/95 $9.50+.00

0008-8846(95)00045-3

HYDRATION PRODUCTS OF ALKALI ACTIVATED SLAG CEMENT

Shao-Dong Wang# and Karen L. Scrivener
Department of Materials, Imperial College of Science, Technology and Medicine,
University of London, London SW7 2BP, UK

#From: Department of Building Materials, Chongqing Institute of
Architecture and Engineering, Chongqing 630045, China

(Refereed)
(Received April 4, 1994; in final form October 26, 1994)

ABSTRACT

This paper presents some recent research on the microstructural development during alkaline activation of slag pastes. Pastes of different slags activated with a range of activators have been prepared and some preliminary results from the study of the pastes activated with sodium hydroxide and waterglass solutions are presented. X-ray diffraction (XRD), differential thermal analysis (DTA), backscattered electron (BSE) imaging of polished samples in the SEM coupled with X-ray microanalysis, and secondary electron imaging of fracture surfaces were used to study the pastes.

This study indicates: (i) that the products form by a dissolution and precipitation mechanism during the early stages of reaction, but at later stages the reaction may continue by a solid state mechanism; (ii) regardless of the activator used, the main hydration product is calcium silicate hydrate with low C/S ratio and varying degrees of crystallinity; (iii) a crystalline phase of hydrotalcite type is formed in slag activated with either NaOH or waterglass; (iv) a crystalline phase of AFm type is also formed in slag activated with NaOH; (v) no hydrates of zeolite group or mica group were formed in slag activated with either NaOH or waterglass solution after wet curing at 20±2 °C up to 15 months or at 80 °C for 14 days.

Introduction

Numerous papers have been published on the use of slag in cement and concrete based on its activation by cement clinker and gypsum. An alternative approach is alkaline activation of slag by group I metal alkalis. Compared with ordinary Portland cement (OPC) and interground slag-blended cement, alkali activated slag (AAS) cement has some advantageous properties, including rapid and high strength development, good durability and high resistance to chemical attack (1-6). Much research on AAS has been done in the Ukraine since the 1950s (5,6). In other countries, interest in alkaline activation of slag has grown markedly during the 1970s. In recent years, AAS cement and concrete have received greater attention world-wide. Some applications, basically on trial, have been carried out in the Far East (2,3,7-10) and in Europe (1,4,11-14). A modified type of AAS cement has been used in small quantities in the USA since 1987 (15-17).

Many aspects of the chemistry of slag hydration activated by alkali are unclear, and this lack of theoretical understanding is impeding the solution of the remaining practical problems obstructing

its wider application. From the literature it appears that the hydrate phases formed depend on the time and temperature of curing and also on the types of slag and activator used, but low-basic calcium silicate hydrate related to tobermorite is always the major hydration product of AAS cement. However the general picture that emerges is one of considerable confusion. Some papers (14,18-20) have reported the presence of calcium hydroxide, C-S-H(II) and a solid solution of magnesium-calcium aluminate hydrate: $(M,C)_4AH_{13}$, but Glukhovsky et al. (5) reported that these phases are not found in AAS pastes; instead they detected some hydrogarnet, zeolitic phases and mica phases, e.g., nepheline, natrolite, analcite, paragonite and gismondite. All these published results are mainly based on XRD techniques, in which some results were misinterpreted. In our recent work using SEM/BSE combined with EDS X-ray microanalysis together with XRD, we found that while C-S-H(I) is the main hydration product regardless of the activator used, some hydrotalcite-type phase is formed as well (21). It is clear that more work on the chemistry of alkali-activated slag hydration is needed. This paper details findings from research addressed at studying the chemistry and microstructural development of slag pastes activated by alkalis.

Experimental

1. Materials

A British slag was used, supplied by Appleby Group Ltd. Its chemical composition was 35.5% SiO_2, 12.6% Al_2O_3, 40.3% CaO, 9.0% MgO, 0.6% Fe_2O_3, 0.5% MnO, 0.7% TiO_2. A small amount of merwinite and a trace of gehlenite were present. The specific surface area was 4100 cm^2/g (Blaine). Alkaline solutions of sodium hydroxide and waterglass (wg) having a SiO_2/Na_2O ratio (i.e. modulus) of 1.0 were made from reagent grade chemicals, with the compositions in grams per 100 ml given in Table 1.

TABLE 1.
Composition of alkaline solutions (grams per 100 ml)

Notation	Formula	Na_2O	SiO_2	Total Solid	pH
4M NaOH	NaOH	12.4	0	12.4	14.6
2M wg(1m)*	$Na_2O{\cdot}SiO_2$	12.4	12.0	24.4	13.4

*where M = concentration in moles/litre; and m = SiO_2/Na_2O (i.e. modulus) of waterglass.

2. Sample Preparation

Ground slag was mixed with the alkaline solutions with liquid:solid ratio of 0.25 (volume of solution in cm3:weight of slag in grammes). The mixes were cast into plastic sample bottles, sealed and cured at 20±2 °C or 80 °C. At the required ages hydration was stopped by freezing in solid CO_2-methanol mixture (–80 °C). The samples were then freeze dried.

3. X-ray Diffraction

For XRD, samples were ground in an agate mortar to a fine powder. A Philips APD/PW1700 Series automatic diffractometer was used with the following conditions: 45 kV, 40 mA, Cu-Kα radiation, 0.050 °2θ step size, at 2 seconds per step.

4. DTA

Samples were prepared as for XRD. A Stanton Redcroft STA-780 series simultaneous thermal analyzer was used with an atmosphere of oxygen-free nitrogen and at a heating rate of 10 °C/min.

5. Scanning Electron Microscopy and Microanalysis

For examinations by the SEM, both secondary electron imaging of fracture surfaces and backscattered electron (BSE) imaging of polished surfaces were used. For the BSE study, the samples were impregnated with epoxy resin, cut into 1-2 mm thick slices, lapped, polished to ¼ μm and then coated with carbon. A JEOL JSM-35CF scanning electron microscope was used, equipped with a solid state backscattered detector and a Link AN 10000 energy dispersive (EDS) X-ray microanalysis system. The contrast in the backscattered electron images depends on the

average atomic number of the area being examined. Phases with a higher average atomic number (e.g. unreacted slag) appear bright and those with a lower average atomic number (e.g. hydrates) appear grey or darker, and the pores appear black.

Microanalyses were carried out at an accelerating voltage of 15 kV for 50 seconds, using reference standards and matrix corrections applied by the ZAF procedure. For hydrate phases, each spot analysed by electron probe relates to a region of some 1 μm across in each direction and phases beneath the sample surface which cannot be seen may be reached by the electron probe. Therefore when the hydrate phases are finely dispersed, X-ray microanalyses may relate to mixtures of phases in varying proportions. Analyses of unhydrated slag were made periodically as a check on the instrument calibration.

Results and Discussion

1. X-ray Diffraction

The XRD traces for the pastes activated with NaOH and with waterglass are shown in Figs. 1 and 2 respectively. The broad and diffuse peak from the original slag around 30-31°2θ reflects the short range order of the CaO-Al_2O_3-MgO-SiO_2 glass structure. At later ages the peak shifts to a slightly smaller value of 2θ due to the formation of C-S-H gel.

For both mixes a peak can be identified, superimposed on the amorphous hump, at about 3.03 Å. This can be attributed to the (110) reflection of poorly crystalline C-S-H(I); it could also be partly due to calcite resulting from carbonation, but there was no evidence of this phase by thermogravimetric analysis. In the pastes activated with NaOH (Fig. 1) this peak can already be identified at 1 day or even earlier ages (21), and by 15 months other peaks from C-S-H(I) can also be identified at 12-13 Å (001), 1.83 Å (020), 1.66 Å (310) and possibly 1.52 Å (220). For the paste cured for 14 days at 80 °C the crystallinity of C-S-H(I) is slightly better than for normal curing for 15 months. In the pastes activated with waterglass (Fig. 2) poorly crystalline C-S-H(I) can only be clearly identified after 7 days, and even after 15 months, only the peaks at 3.03 and possibly 1.82 Å can be identified; but for the paste cured at 80 °C for 14 days the peaks at 1.82 and 1.66 Å can also be identified. Comparing Fig. 1 with Fig. 2, it is clear that hydration products formed in NaOH-slag pastes are more highly crystalline than those formed in waterglass-slag pastes

In the pastes activated with NaOH (Fig. 1) there are also peaks at 7.64, 3.82, 2.57, 2.28 and 1.94 Å, which correspond to those of hydrotalcite given by Gastuche et al. (22). They can be indexed as the (003), (006), (012), (015) and (018) reflexions, with the lattice parameters **a** = 3.04 Å and **c** = 22.92 Å. Only after 28 days can the peak at 7.64 Å be identified in the pastes activated with waterglass solution; with the second peak at 3.86 Å appearing after one year (Fig. 2). Hydrotalcite itself is a natural mineral with the formula $Mg_6Al_2CO_3(OH)_{16}{\cdot}4H_2O$ and has a structure based on brucite-type layers with interlayer water molecules and CO_3^{-2} ions. Many other anions can occupy the interlayer positions leading to changes in the cell parameters. Phases of this type have previously been identified in pastes of Portland cement/slag blends (23-26). Although the Mg/Al ratio for the natural mineral is 3, ratios from 2 to 3 have been found in cementitious systems (21,25,26). Gastuche et al. (22) found that changes in the Mg/Al ratio of hydrotalcite-type phases also had an effect on the cell parameters. Those found here agree well with those of the 3R polytype identified by Gastuche at al. (22).

The SEM, EDS and DTA results described below indicate the presence of an AFm phase. Peaks expected for this phase are difficult to distinguish in the XRD patterns, but shoulders at d = 7.92-8.00 and 3.94 Å could be seen to the left of the peaks at d = 7.64 and 3.82 Å in paste activated with NaOH (Fig. 1). These correspond to the two main peaks of the AFm-type phase, C_4AH_{13}.

No hydrates of zeolite or mica groups such as nepheline, natrolite, analcite, paragonite and gismondite and no other crystalline phases containing alkali cations could be identified in the XRD

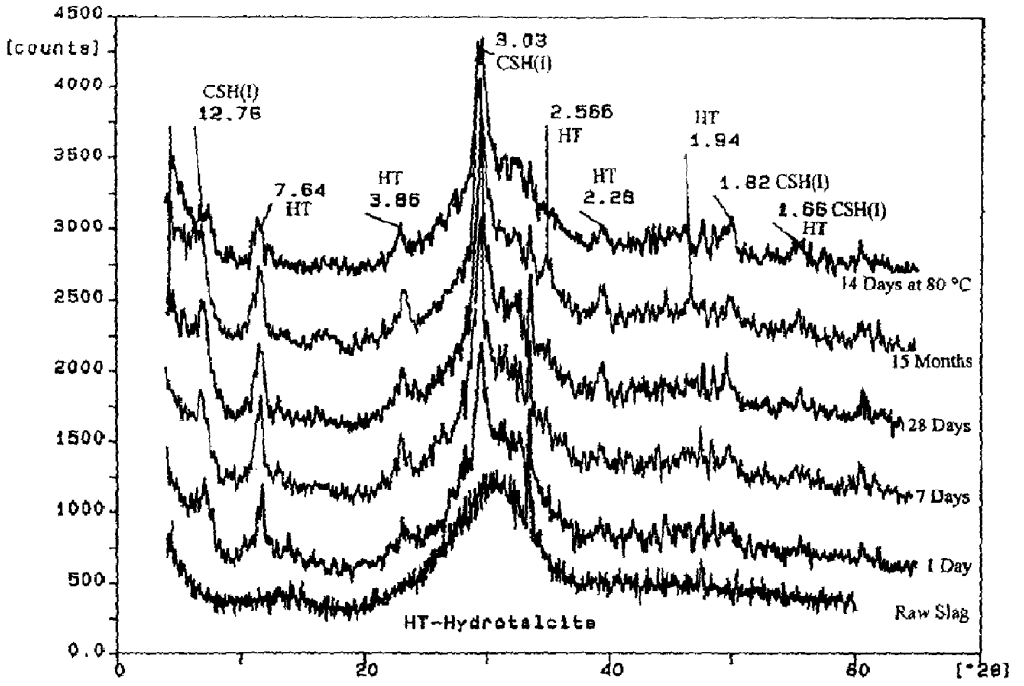

Fig. 1 XRD patterns of slag pastes activated with 4M NaOH solution.

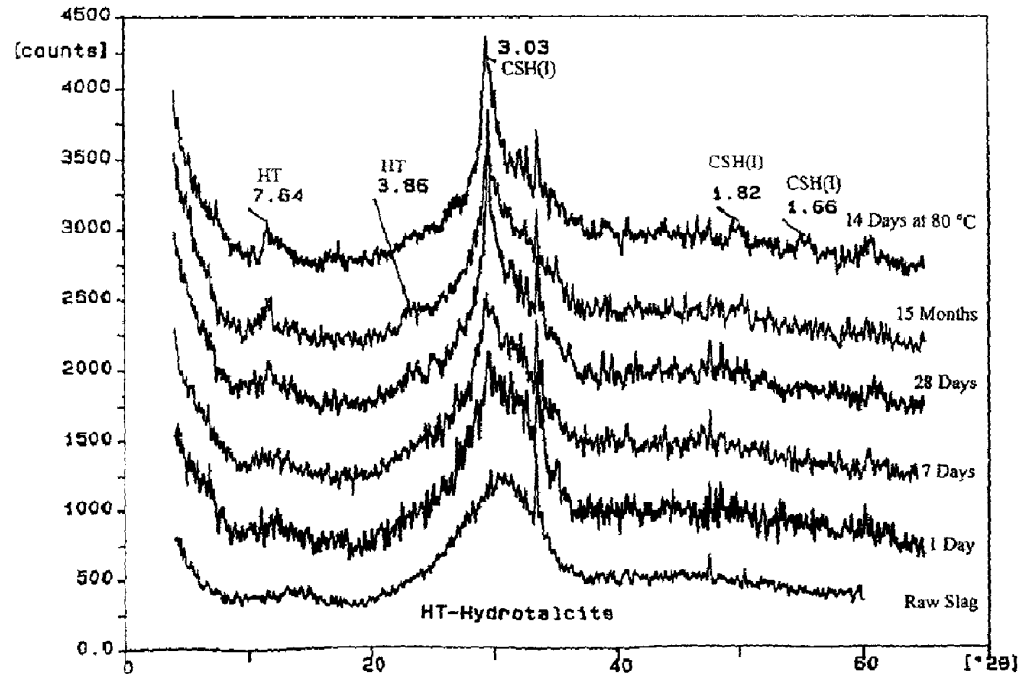

Fig. 2 XRD patterns of slag pastes activated with 2M wg(1m) waterglass solution.

traces of the pastes activated with either NaOH or waterglass up to 15 months of age after normal wet curing at 20±2 °C or at 80 °C for 14 days. Neither were C-S-H(II) and $Ca(OH)_2$ found in the AAS pastes. There appears to be no convincing evidence for the existence of a $(M,C)_4AH_{13}$ solid solution as postulated by some investigators.

2. DTA Results

Figs. 3 and 4 show the DTA curves for pastes activated with NaOH and waterglass solution respectively. In both patterns the endothermic peak at 90-110 °C is due to C-S-H(I). For pastes activated with NaOH (Fig. 3), the shoulder at about 130-170 °C, superposed on the right side of the main peak, indicates the presence of an AFm-type phase; but for pastes activated with waterglass (see Fig. 4), this peak can not be distinguished. The presence of the peak at 330-400 °C in both DTA patterns can be attributed to the hydrotalcite-type phase. DTA traces for hydrotalcite-type phases reported by Gastuche et al. (22) showed a large peak at 330-360 °C, corresponding to the release of structural water and CO_2.

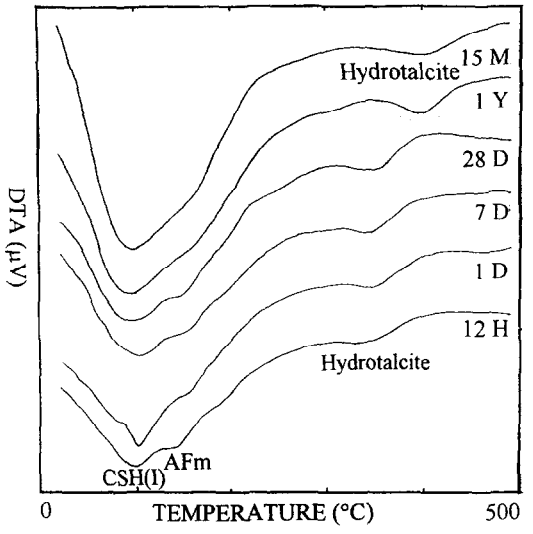

Fig. 3 DTA patterns of slag activated with 4M NaOH showing endothermic peaks from CSH(I), AFm and hydrotalcite type phases.

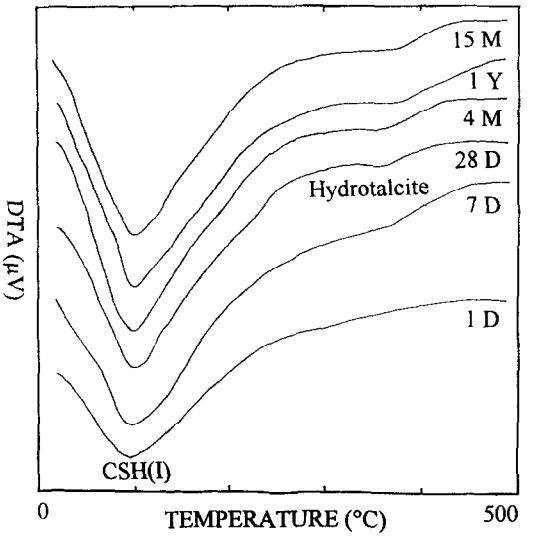

Fig. 4 DTA patterns of slag activated with 2M wg(1m) showing endothermic peaks from CSH(I) and hydrotalcite-type phase.

3. SEM Observations

Figs. 5-10 show micrographs of pastes activated with 4M NaOH and 2M wg(1m) at different ages. In samples at early ages (Figs. 5-8) it is apparent that hydration products have formed in the space between the slag grains, originally occupied by alkaline solution, indicating their formation by a dissolution and precipitation mechanism at early ages. In the pastes activated with waterglass (Figs. 6,8,10) all the products have a homogeneous, amorphous appearance and it is not possible to resolve different phases in the SEM images. With NaOH (Figs. 5,7), however, distinct plates about 0.1-0.2 μm thick and up to 15 μm in diameter could be identified.

As noted previously (21) dark rims up to 0.5-1 μm thick around slag particles were formed after 5-7 days. From Figs 7-10 it can be seen that the rims become clearer and thicker with ageing. Similar rims have been observed around slag particles hydrating in Portland cement/slag blends (26). The presence of the rims suggests that the slag particles may form some in-situ products by a solid state mechanism at later ages. Discrete crystals of the hydrotalcite-type phase could not be differentiated by the SEM images, but previous studies of OPC-slag blend pastes by Richardson et al. (26) by TEM found sub-micrometer sized crystals of this phase dispersed through C-S-H.

Fig. 5 SEM images for slag paste activated with NaOH at 1 day. Left - secondary electron image of fracture surface, Right - backscattered electron image of polished surface, showing the platy AFm-type phase mixed with CSH(I).

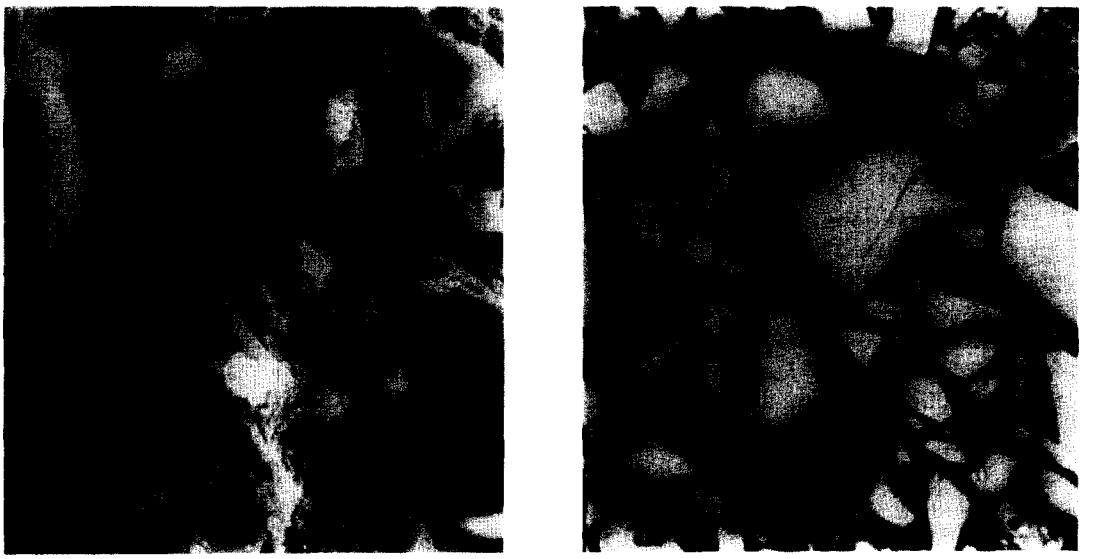

Fig. 6 SEM images for slag paste activated with waterglass at 1 day. Left - secondary electron image of fracture surface, Right - backscattered electron image of polished surface, showing the homogeneous, amorphous appearance of poorly crystalline CSH(I).

Fig. 7 BSE image for slag paste activated with NaOH at 7 days, showing the platy AFm-type phase mixed with CSH(I).

Fig. 8 BSE image for slag paste activated with waterglass at 5 days, showing a slag particle leaving the crystalline phase unreacted.

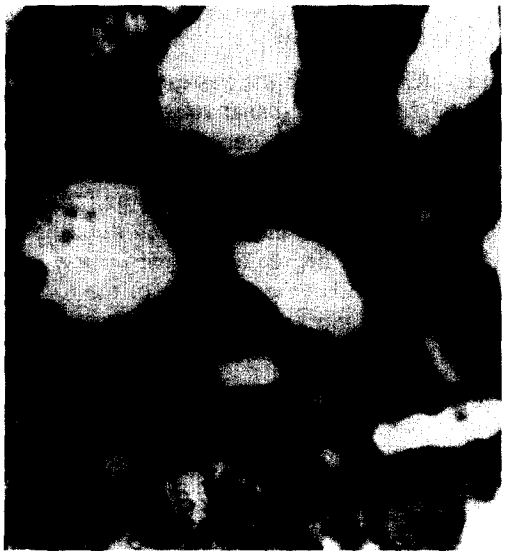

Fig. 9 BSE image for slag paste activated with NaOH at 1 year, showing clearly the "rims" around slag particles and their darker appearance than "general" products.

Fig. 10 BSE image for slag paste activated with waterglass at 1 year, showing clearly the "rims" around slag particles and their darker appearance than "general" products.

Fig. 8 shows a slag particle with crystalline material dispersed in the glass. At the edge of this particle the glassy phase has dissolved leaving the crystalline phase unreacted, indicating the big difference in reactivity between these phases and the approximate thickness of the reacted layer of slag particles at this age.

4. X-ray Microanalysis (EDS)

Some of the microanalyses were of materials present in clearly defined parts of the microstructure as slag "rims" or "platy" crystals. Others were of material present in the matrix; these will be described as "general" analyses.

The microanalyses confirmed that the major hydration product was C-S-H in all samples. In addition to Ca and Si, amounts of Na, Mg, Al and S were also found in all the analyses. Of the species detected, sodium is the only one which is likely to be present in significant quantities in the solution. During specimen preparation, species dissolved in the solution will precipitate out on the surface of the hydration products. Some of the free alkali may be removed from the specimen while cleaning and polishing. Consequently it has so far been impossible to gain an accurate appraisal of the degree of sodium incorporation in the hydration products.

Fig. 11 shows a plot of the Mg/Ca vs Al/Ca ratios for the waterglass-slag pastes hydrated for one year. There is a clear linear relationship between the two ratios with the points lying on a line with Mg/Al ratio of 2.2. This relationship is consistent with the view that the analyses are mixtures of C-S-H with small crystals of hydrotalcite-type phase dispersed through the C-S-H as suggested by the X-ray examination. Analyses from rims around slag grains can be seen to contain a much higher proportion of the hydrotalcite-type phase, which accounts for their darker appearance in the BSE images.

Extrapolating the straight line to Mg/Ca = 0 indicates that the C-S-H gel also contains a significant proportion of aluminium (Al/Ca $\approx$ 0.22) either in solid solution within the C-S-H structure or in an AFm form finely intermixed with it. Richardson et al. (26) have shown that in slag/cement pastes cured at an elevated temperature Al can replace the bridging Si in the dreierketten C-S-H structure. Therefore in pastes hydrated for 1 year (when the degree of polymerization is relatively high) the majority of this aluminium may be in solid solution in the C-S-H structure.

In Figs. 12 and 13 the Mg/Ca ratios are plotted against Al/Ca ratios for the pastes activated with NaOH at 1 day and 1 year, respectively. The general analyses show a similar relationship to that seen in the paste activated with waterglass. As before this is taken as evidence that the analyses came from areas of paste which are mixtures of C-S-H with hydrotalcite-type phase. Extrapolating to Mg/Ca = 0 indicates that the ratio Al/Ca in the C-S-H is 0.16 at 1 day and 0.20 at 1 year. While it may be feasible that this level of aluminium could be accommodated in bridging sites in the silicate chains at the later age, it seems unlikely that the degree of polymerization at 1 day would be sufficient for the aluminium to be accommodated within the structure of the C-S-H itself. In this case, at least, it is more likely that the aluminium exists in AFm type layers intermixed with the C-S-H type layers as described in Taylor's C-S-H gel model (23,24).

An additional feature of pastes activated with NaOH is the group of analyses centered on the platy crystals seen in the micrographs. These show a different relationship, lying on a line extending from that of mixtures of C-S-H and hydrotalcite-type phase to a point on the Al/Ca axis with a value of 0.5 (the ratio expected of the AFm type phase: C_4AH_{13}). Taken together with the X-ray and DTA evidence this clearly indicates that the platy phase is C_4AH_{13}.

If the analyses from all points are corrected for the aluminium associated with the hydrotalcite-type phase, a new graph can be plotted to show the relationship between the aluminium and calcium in the C-S-H and AFm phases (Fig. 14). This indicates that the ratio Al/Ca is always around 0.5 confirming the identification of the plates as AFm and indicating a similar relationship for the calcium and aluminium within the 'C-S-H gel'. This strongly supports the view that, at

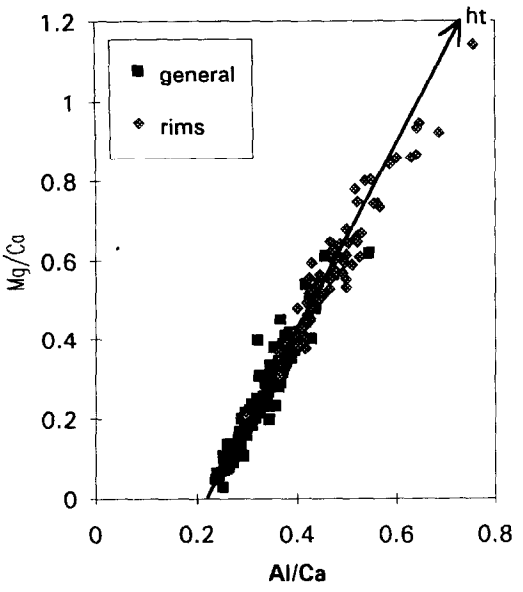

Fig. 11 Plot of Mg/Ca vs Al/Ca for slag activated with waterglass hydrated for 1 year. The linear relationship proves the presence of a hydrotalcite-type phase (ht). "Rims" contain more ht than "General" hydration products.

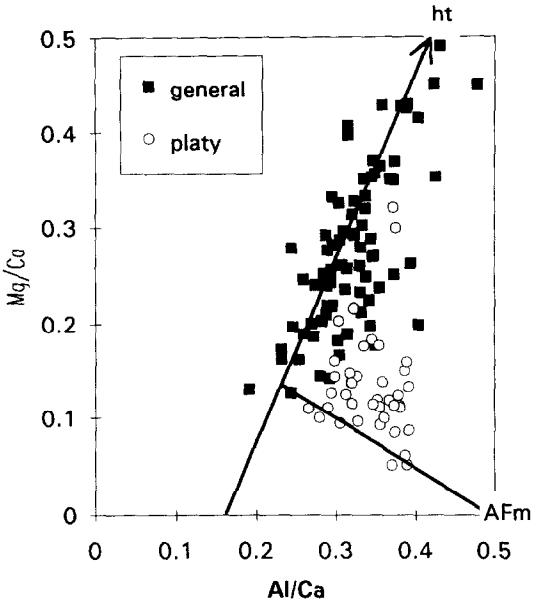

Fig. 12 Plot of Mg/Ca vs Al/Ca for slag activated with NaOH at 1 day, showing mixtures of CSH, an AFm-type phase and a hydrotalcite-type phase.

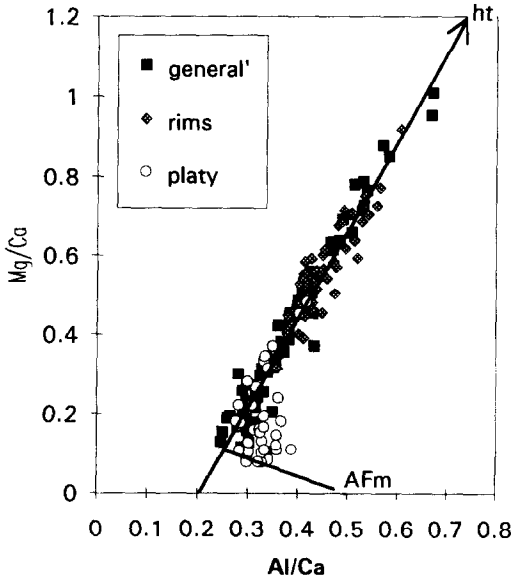

Fig. 13 Plot of Mg/Ca vs Al/Ca for slag activated with NaOH at 1 year, showing the presence of CSH, an AFm-type phase and a hydrotalcite-type phase

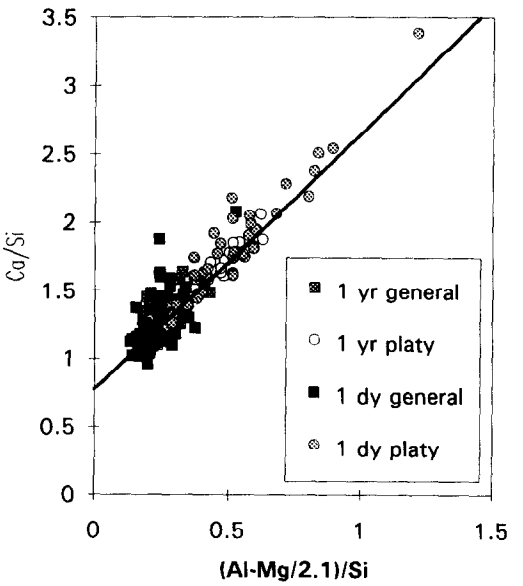

Fig. 14 Plot for slag activated with NaOH at 1 day and 1 year, corrected for the aluminium associated with the hydrotalcite-type phase.

least initially, the aluminium within the gel exists as AFm layers; although at later ages it may become incorporated into the C-S-H structure in bridging positions linking dimeric silicate units.

Conclusions

1 During the hydration of AAS cements, the products form by a dissolution and precipitation mechanism during the early stages of reaction. At later stages the presence of rims around the slag grains suggests that reaction may continue by a partially solid state mechanism.
2 Regardless of the activator used, the main hydration product is calcium silicate hydrate with a low Ca/Si ratio. With NaOH some semi-crystalline C-S-H(I) is formed even at early ages. When waterglass is used the degree of crystallinity is very low even at one year.
3 A hydrotalcite-type phase is formed in the pastes activated with both NaOH and waterglass on a sub-micrometer scale such that it cannot be distinguished in the SEM images.
4 A crystalline phase of AFm type is formed in slag paste activated with NaOH. This phase can be identified as plates 0.1-0.2 μm thick and up to 15 μm in diameter.
5 No phases of the zeolite or mica groups such as, natrolite, analcite, paragonite and gismondite and no other crystalline phases containing alkali cations could be identified in these pastes activated with either NaOH or waterglass solution up to 15 months of age under normal wet curing at 20±2 °C or at 80 °C for 14 days.
6 There appears to be no convincing evidence for the existence of a $(M,C)_4AH_{13}$ solid solution as postulated by some investigators.

Acknowledgements

We would like to thank Prof. H.F.W. Taylor for helpful discussions and particularly for help in the interpretation of the XRD patterns, and Mr R. Sweeney for assistance in the use of diffractometer. SDW is very grateful to The Institution of Mining and Metallurgy, UK for the award of a Stanley Elmore Fellowship, to The Committee of Vice-Chancellors and Principals and Imperial College for the award of an Overseas Research Studentship and to Prof. P.L. Pratt for his recommendations in the above applications and for much additional assistance.

References

ICCC = International Congress on the Chemistry of Cement.
ICFSSNC = International Conf. on Fly Ash, Silica Fume, Slag and Natural Pozzolans in Concrete.

1. B. Talling and J. Brandstetr, 3rd ICFSSNC, Trondheim, SP114-74, **2**, 1519-46(1989).
2. S.D. Wang, Mag. Concr. Res., **43**(154), 29-35(1991).
3. X.C. Pu, C.C. Gan, S.D. Wang and C.H. Yang, Reports of research on alkali-activated slag cement and concrete; Chongqing Inst. of Archit. and Eng., China, 1988, 6 vols. (in Chinese).
4. R. Andersson, H-E Gram, J. Malolepszy and J. Deja, Alkali-activated slag; Swedish Cem. Conc. Res. Inst., 104ps, Stockholm, 1988.
5. V.D. Glukhovsky, G.S. Rostovskaja and G.V. Rumyna, 7th ICCC, Paris, **III**, V164-V168(1980).
6. V.D. Glukhovsky, Silic. Ind., **48**(10), 197-200(1983).
7. X.C. Pu, C. Gan & J. Chen, Proc. Inter. Symp. Concr. Eng., Nanjing, **2**, 1144-49(1991).
8. I.V. Belitsky, A. Sakata, T. Kado and S. Goto, 3rd Beijing Inter. Symp. Cem. Concr., Beijing, **2**, 1028-31(1993).
9. I.V. Belitsky, A. Sakata, T. Kado and S. Goto, 3rd Beijing Inter. Symp. Cem. Concr., Beijing, **2**, 1038-1042(1993).
10. S-Y Hong, J-C Kim and J-K Kim, 3rd Beijing Inter. Symp. Cem. Concr., Beijing, **2**, 1059-1063(1993).
11. M.A. Smith and G.J. Osborne, World Cement Technology, Nov/Dec, 223-233(1977).
12. B. Fross, Silic. Ind., **48**(3), 79-82(1983).

13.W. Brylicki, J. Malolepszy and S. Stryczek, 9th ICCC, New Delhi, **3**, 312-318(1992).
14.B. Talling, 3rd ICFSSNC, Trondheim, SP114-72, **2**, 1485-1500(1989).
15.D.M. Roy, M.R. Silsbee and D. Wolfe-Confer, Mat. Res. Soc. Symp. Proc., **179**, 203-218(1991).
16.D.M. Roy, M.R. Silsbee, Mat. Res. Soc. Symp. Proc., **245**, 153-164(1992).
17.W.J. Clarke and M. Helal, Mat. Res. Soc. Symp. Proc., **179**, 219-232(1991).
18.Q.H. Cheng, A. Tagnit-Hamou and S.L. Sarkar, Mat. Res. Soc. Symp. Proc., **245**, 49-54(1992).
19.A. Roy, P.J. Schilling, H.C. Eaton and P.G. Malone et al., J. Am. Ceram. Soc., **75**(12), 3233-40(1992).
20.R. Dron, H. Hormain and P. Petit, C. R. Seances. Acad. Sci., Ser. C, **280**, 187-88(1975).
21.S.D. Wang and K.L. Scrivener, 3rd Beijing Inter. Symp. Cem. Concr., Beijing, **2**, 1047-53(1993).
22.M.C. Gastuche, G. Brown and M.M. Mortland, Clay Minerals, **7**, 177-192(1967).
23.H.F.W. Taylor, Cement Chemistry, p. 167, Academic Press, London, 1990.
24.H.F.W. Taylor, Adv. Cem. Based. Mats., **1**(1), 38-46(1993).
25.A.M. Harrisson, N.B. Winter and H.F.W. Taylor, Mat. Res. Soc. Symp. Proc., **86**, 199-208(1986).
26.I.G. Richardson and G.W. Groves, J. Mat. Sci., **27**(22), 6204-6212(1992).